

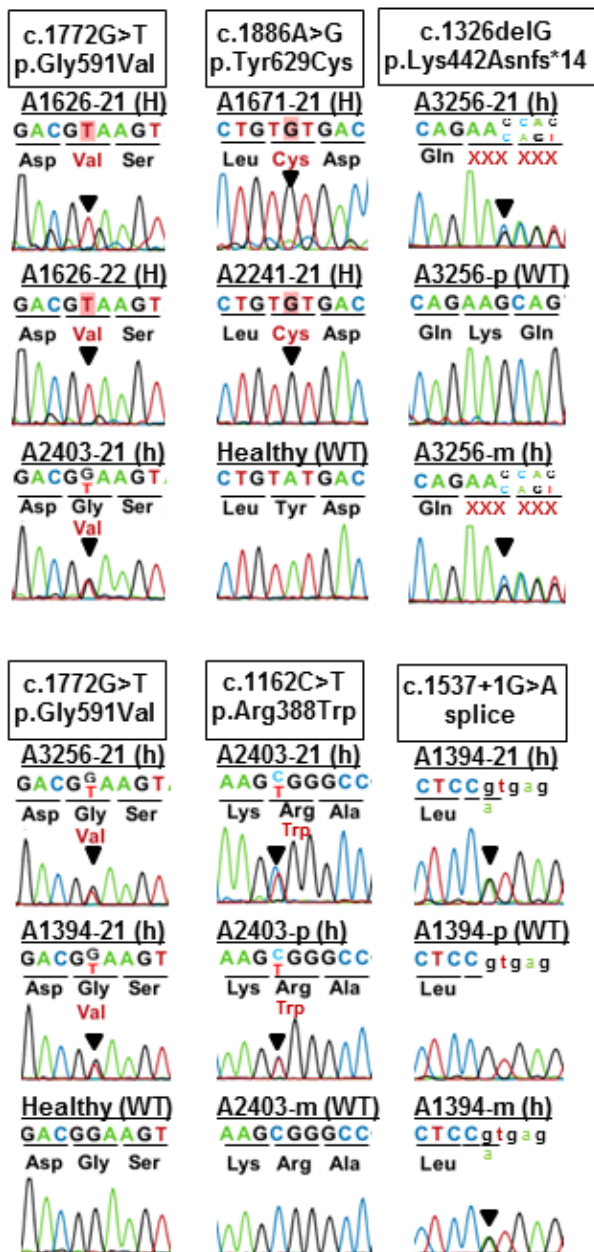
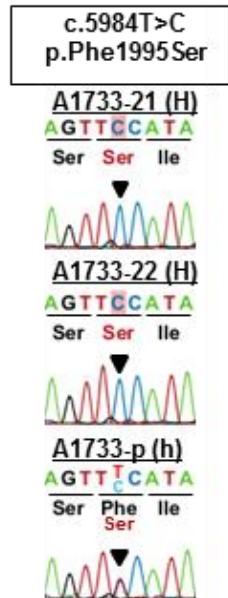
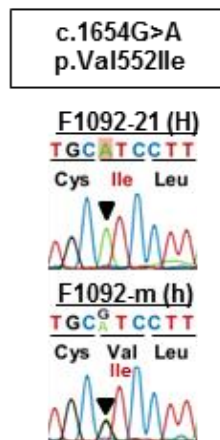
Supplementary Figure 1. Homozygosity mapping and WES identify *NUP93* mutations in 2 additional families with steroid resistant nephrotic syndrome.

(A) Homozygosity mapping identifies recessive candidate loci. In 2 families with nephrotic syndrome, A1626 and A2241, non-parametric lod scores (NPL) were calculated and plotted across the human genome. The x-axis shows Affymetrix 250K *Styl* array SNP positions on human chromosomes concatenated from *p*-ter (left) to *q*-ter (right). Genetic distance is given in cM. Maximum NPL peaks (red circles) indicate candidate regions of homozygosity by descent. The *NUP93* locus (arrowhead) is positioned within one of the maximum NPL peaks on chromosome 16q.

(B) Primer location for RT-PCR analysis of an individual with a splice site mutation in *NUP93* (red and blue arrows, referring to **(C)** and **(D)**, respectively).

(C-D) RT-PCR analysis of the *NUP93* transcript in patient A1394-21 harboring the c.1537+1G>A mutation in intron 13 and control individual using primers located in exons 11 and 14 **(C)**, and exons 12 and 14 **(D)**. In addition to the wildtype bands of 518 bp **(C)** or 405 bp **(D)** corresponding to normal splicing, bands of 326 bp **(C)** and 213 bp **(D)**, respectively, were detected in cDNA of individual A1394-21

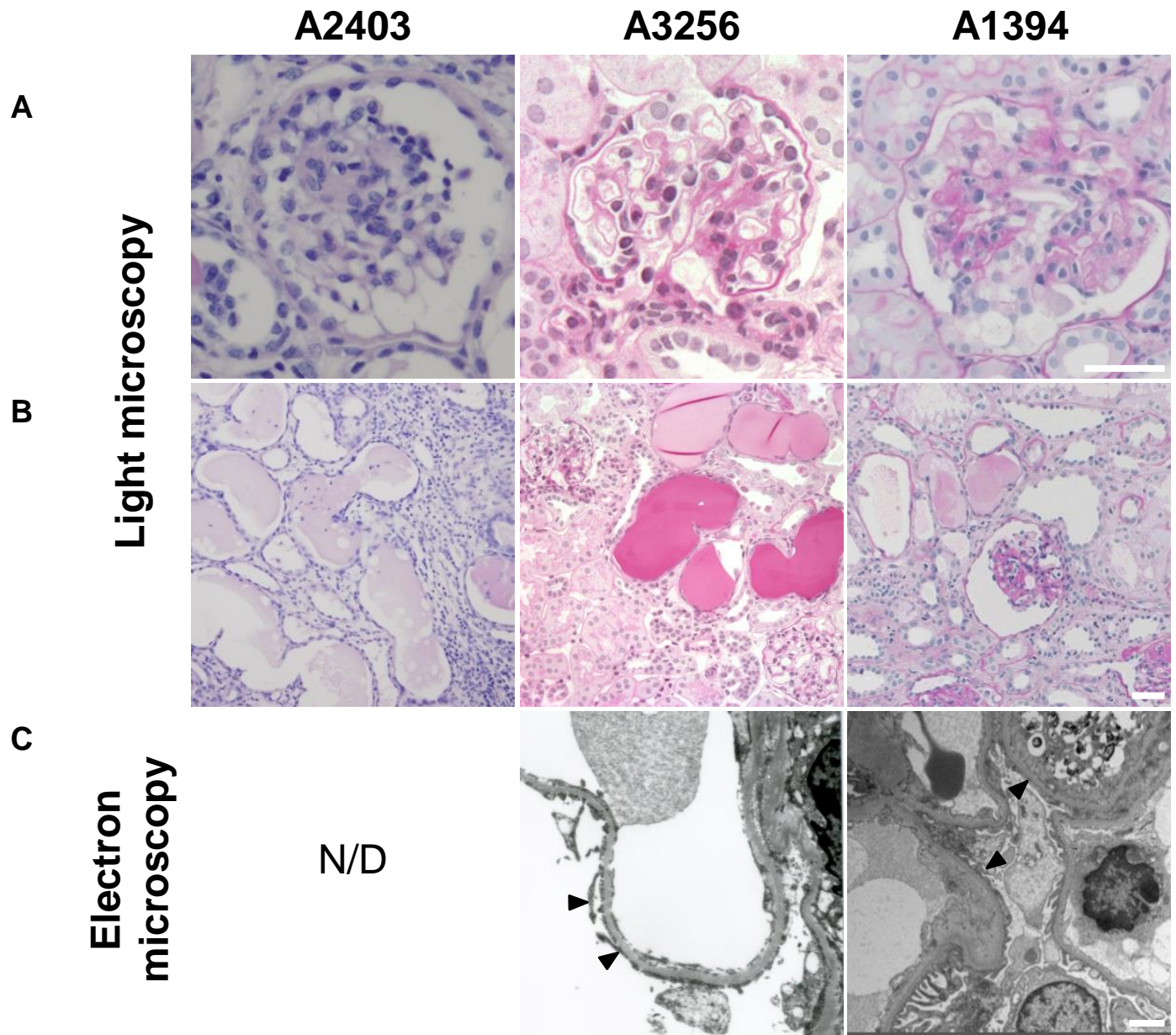
(E) Sanger sequencing of RT-PCR product from A1394-21 revealed that the c.1537+1G>A mutation leads to aberrant splicing, with in-frame skipping of exon 13 (192 bp).

A**NUP93****B****NUP205****C****XPO5**

Supplementary Figure 2. Sequencing traces of individuals with mutations in *NUP93* (A), *NUP205* (B), and *XPO5* (C).

Sanger sequencing traces are shown for 10 individuals from 8 families with mutations in *NUP93* (A), *NUP205* (B), and *XPO5* (C). Arrowheads denote altered nucleotides.

p, paternal; m, maternal; WT, wildtype.



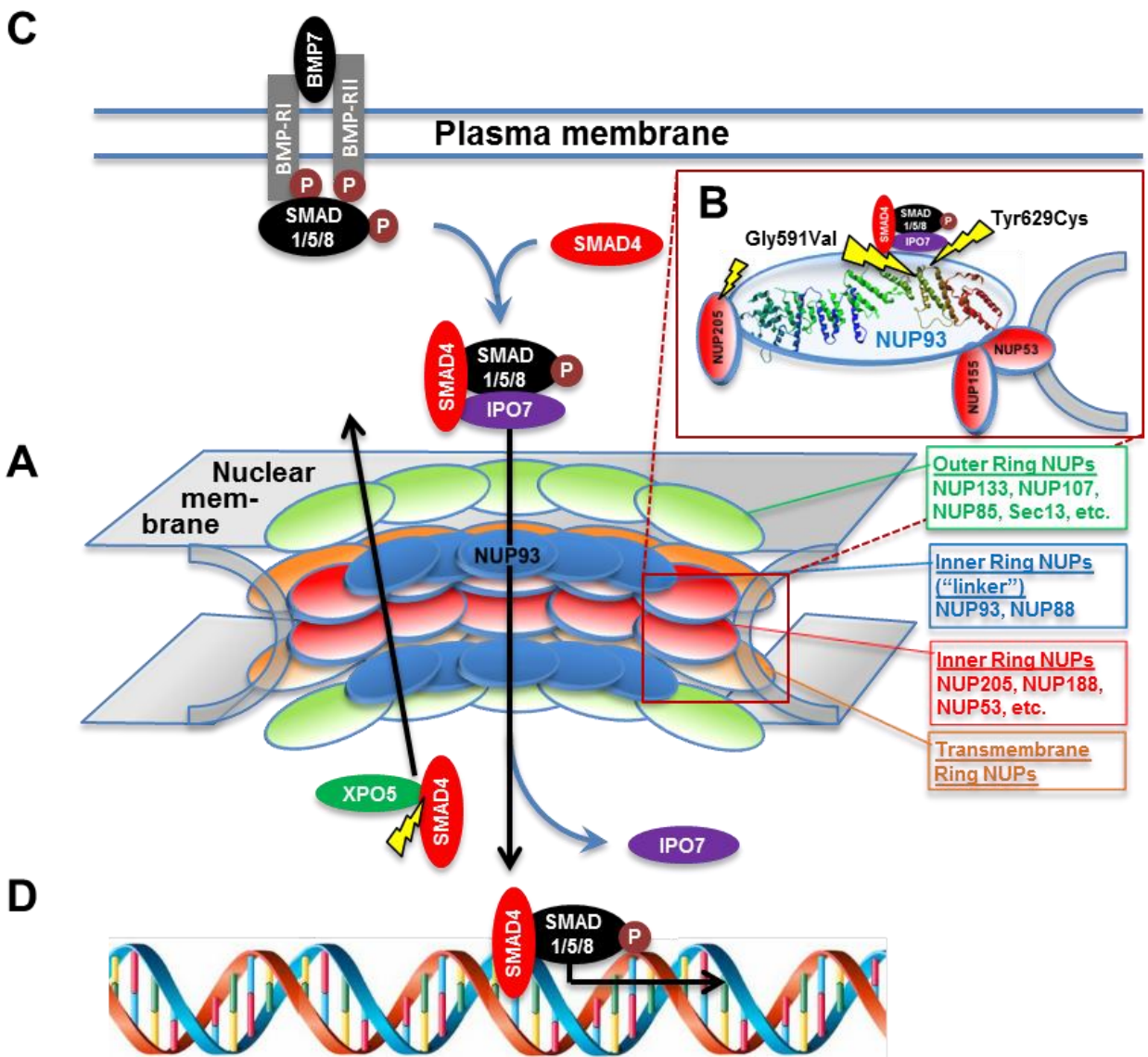
Supplementary Figure 3. Renal histologies of individuals A2403, A3256, and A1394 with recessive mutations in *NUP93*.

(A) H&E staining at high magnification (63x) shows diffuse mesangial sclerosis in A2403-21, and focal-segmental glomerulosclerosis in A3256-21 and A1394-21.

(B) H&E staining at low magnification (40x) reveals tubular atrophy, tubular dilation with protein casts, and cysts with interstitial infiltrations.

(C) Transmission electron microscopy images show partial foot process effacement (arrowheads). (magnification $\times 15,000$); N/D, not data.

Scale bars are 30 μm (**A**, **B**) and 2 μm (**C**).



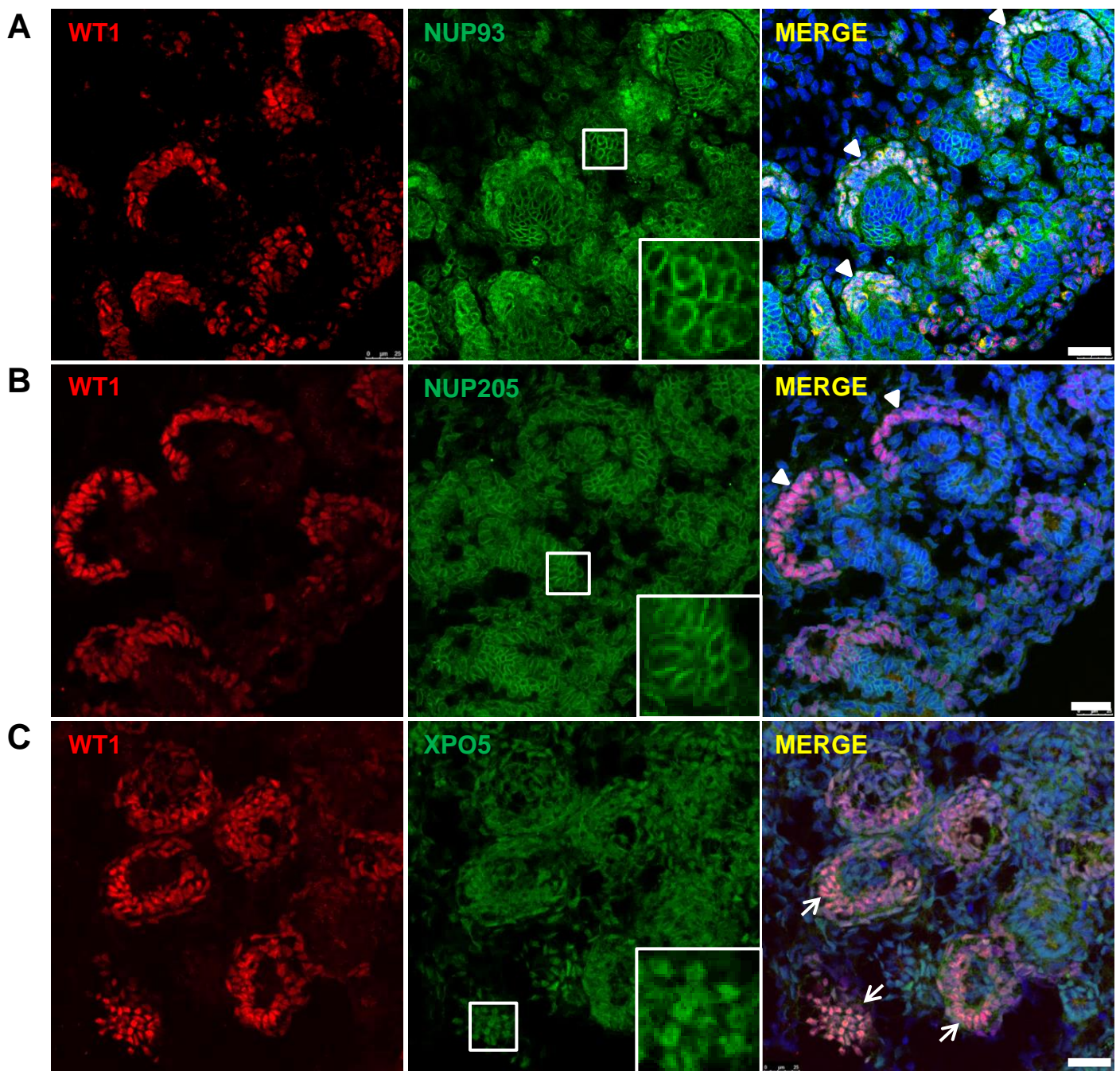
Supplementary Fig. 4. Interaction of nuclear pore complex (NPC) proteins NUP93 and NUP205 with SMAD, importin7 (IPO7), and exportin5 (XPO5) showing positions of mutations that abrogate interactions.

(A) Subcomplexes of the NPC are depicted and labeled in different colors.

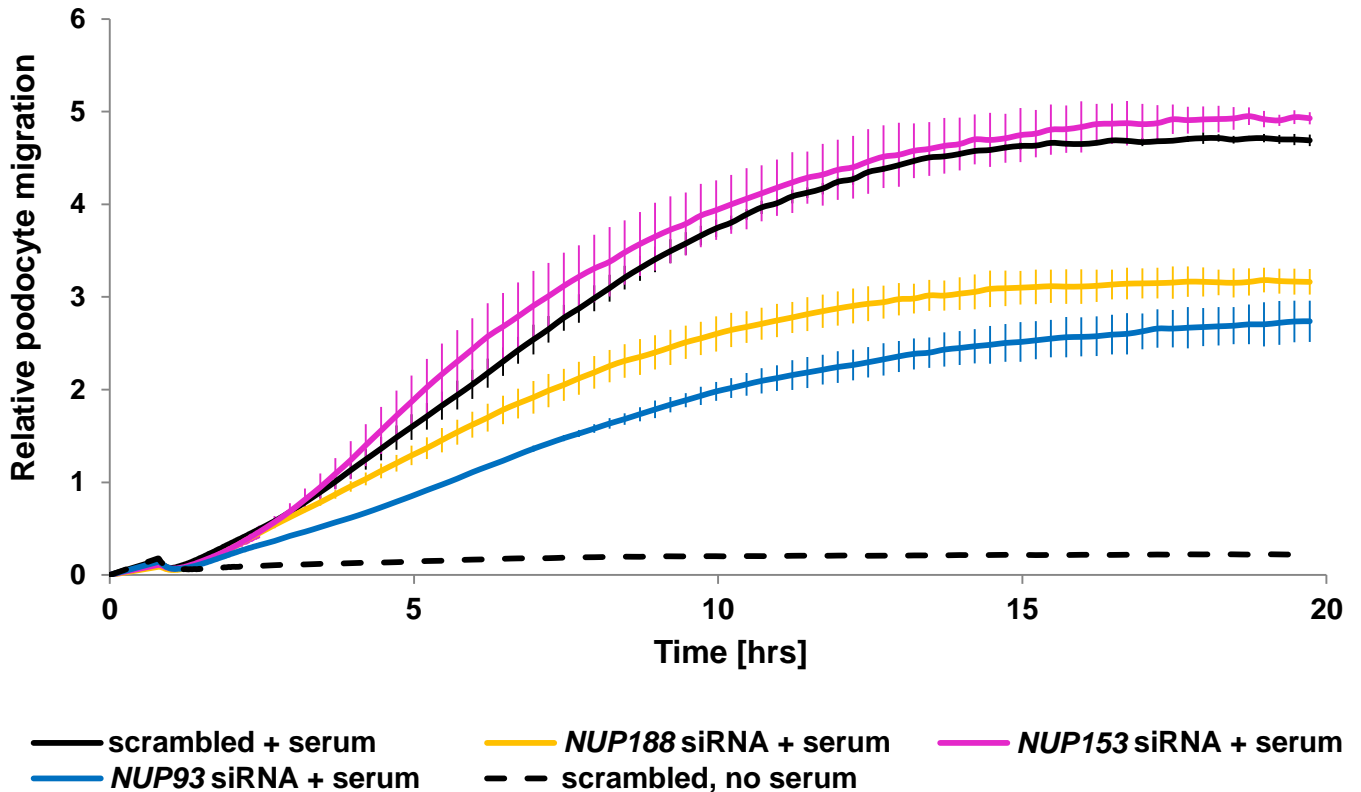
(B) Inset from (A): NUP93 and NUP155 are tethered to the nuclear membrane by NUP53. 3D structure of NUP93 is shown in relation to likely positions of interaction with NUP205, IMP7 or SMADs. Position of NUP93 and NUP205 mutations that abrogate the interaction and were found in individuals with SRNS are marked by yellow lightning signs.

(C) BMP7 binding to its receptor causes phosphorylation of SMAD1/5/8, resulting in dissociation from the receptor and binding to SMAD4. The SMAD4/1/5/8 complex interacts with importin7, enabling the SMAD complex to enter the nucleus through the NPC via NUP93 interaction, bind to cognate DNA sites, and initiate transcription of SMAD downstream targets.

(D) XPO5 binds to SMAD4 for nuclear export. Deletion of the nuclear export signal of SMAD4 abrogates interaction with XPO5.

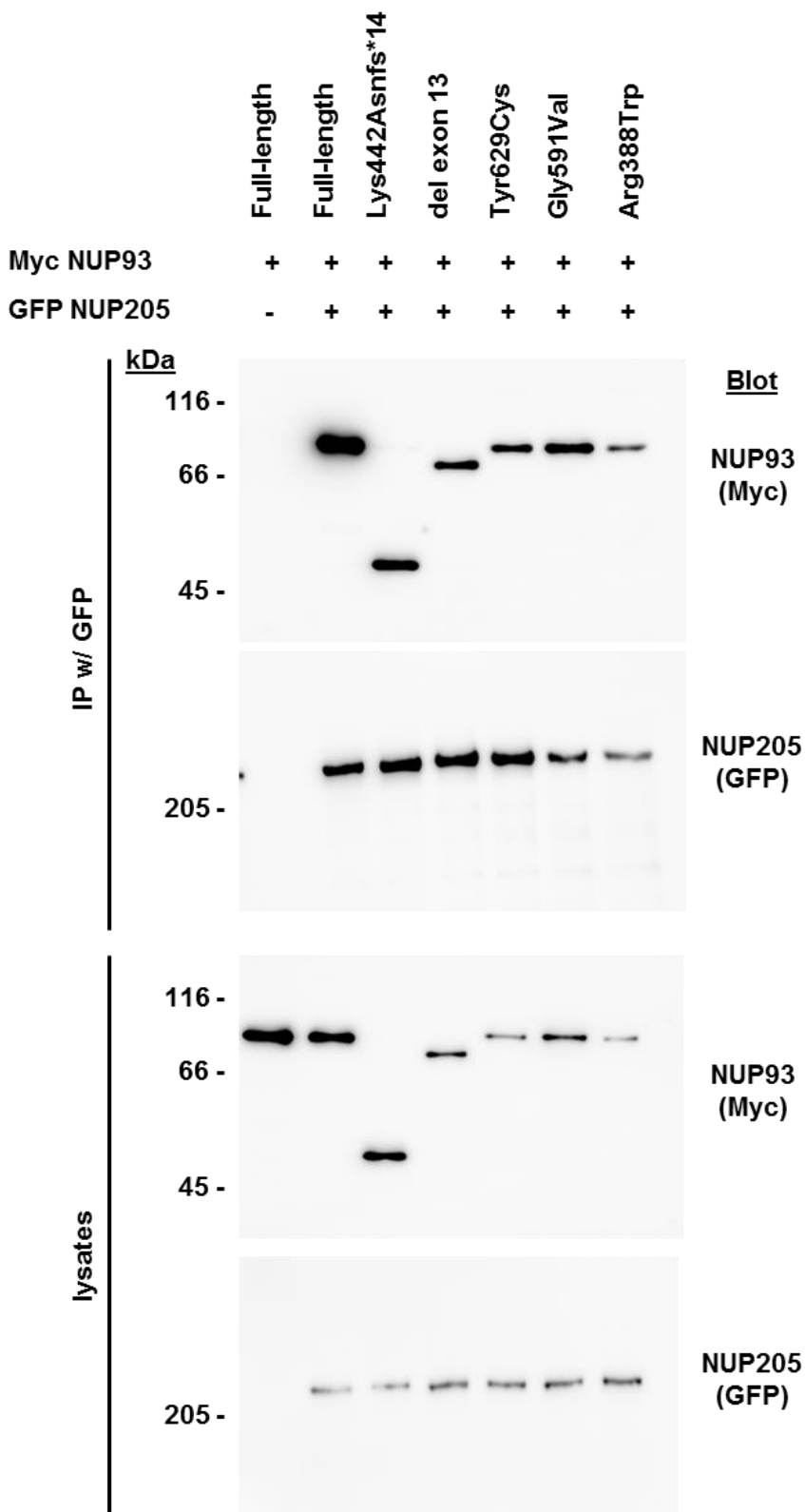


Supplementary Figure 5: NUP93, NUP205, and XPO5 localize to developing podocytes. (A-C) Neonatal rat coronal kidney sections at embryonic day 16.5 p.c. were stained with antibodies against NUP93, NUP205 or XPO5 (green) and the podocyte nuclear marker WT1 (red). Note that NUP93 (A) and NUP205 (B) mark nuclear envelopes with a nuclear rim pattern in podocyte precursor cells (arrow heads) at the capillary loop stage and in other cell types in developing kidney. Anti-XPO5 antibody (C) prominently marks nuclear content of cells in developing kidney with a dot-like pattern (arrow). Scale bars are 25 μ m.



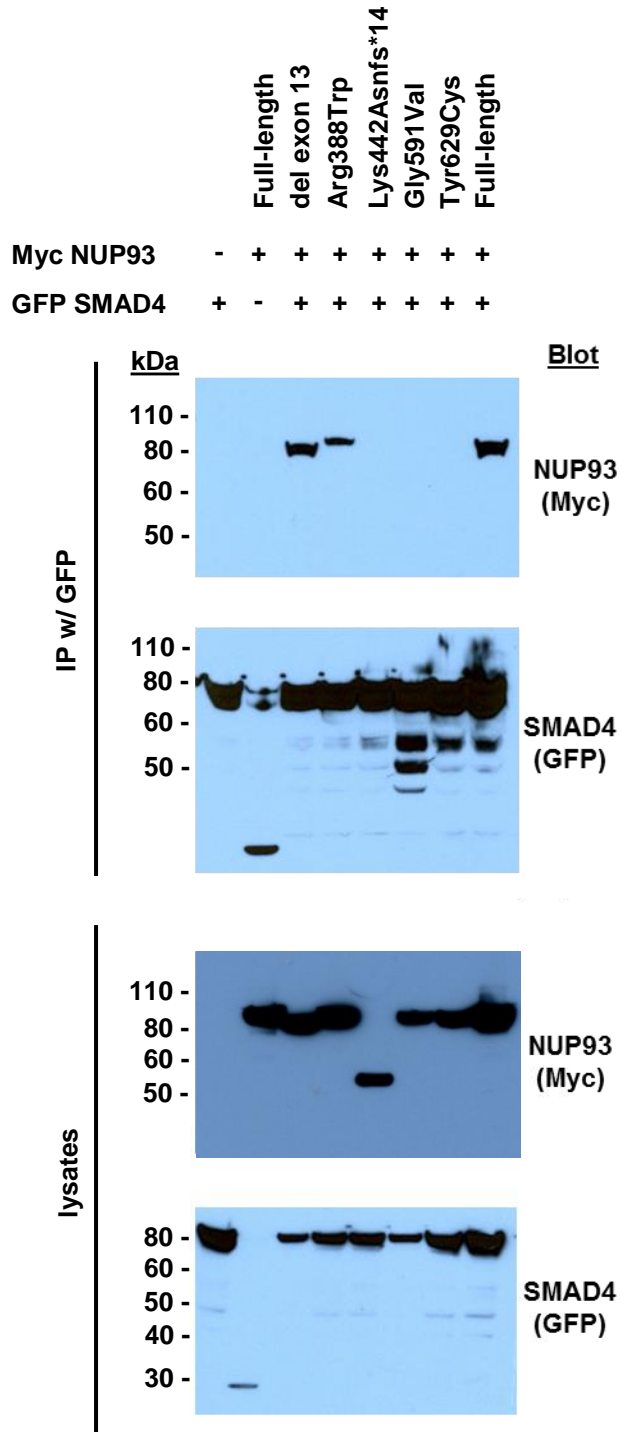
Supplementary Figure 6: Knockdown of *NUP93* and its interactor *NUP188*, but not *NUP153* impair the migratory phenotype of human podocytes *in vitro*.

Compared to basal migration rate (dotted black line), the migration rate of human podocytes is increased following administration of serum as a chemoattractant (solid black line). Knockdown of *NUP93* impairs podocyte migration rate *in vitro* (blue line). Knockdown of *NUP188*, encoding a direct interaction partner of *NUP93* causes a similar, but less pronounced reduction in cell migration rate (yellow line). In contrast, knockdown of the gene encoding the nuclear basket protein *NUP153*, does not affect cell migration (purple line).



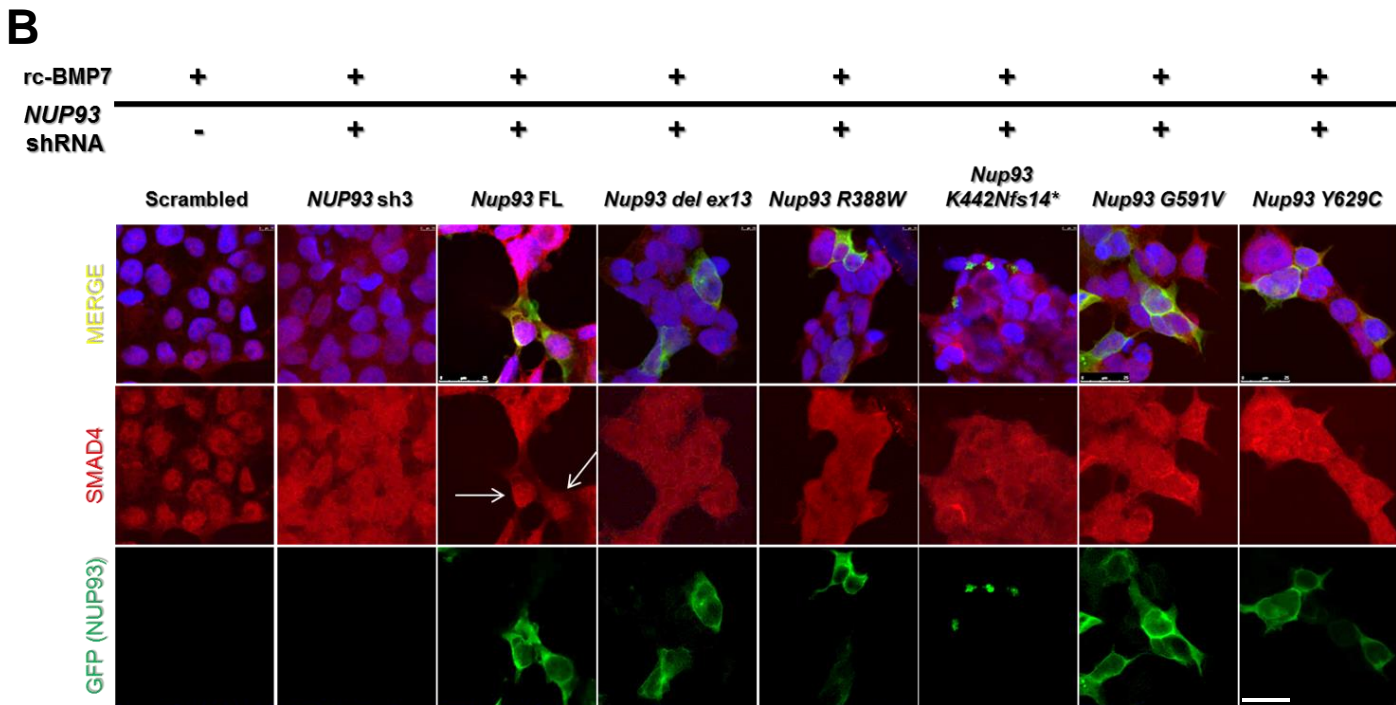
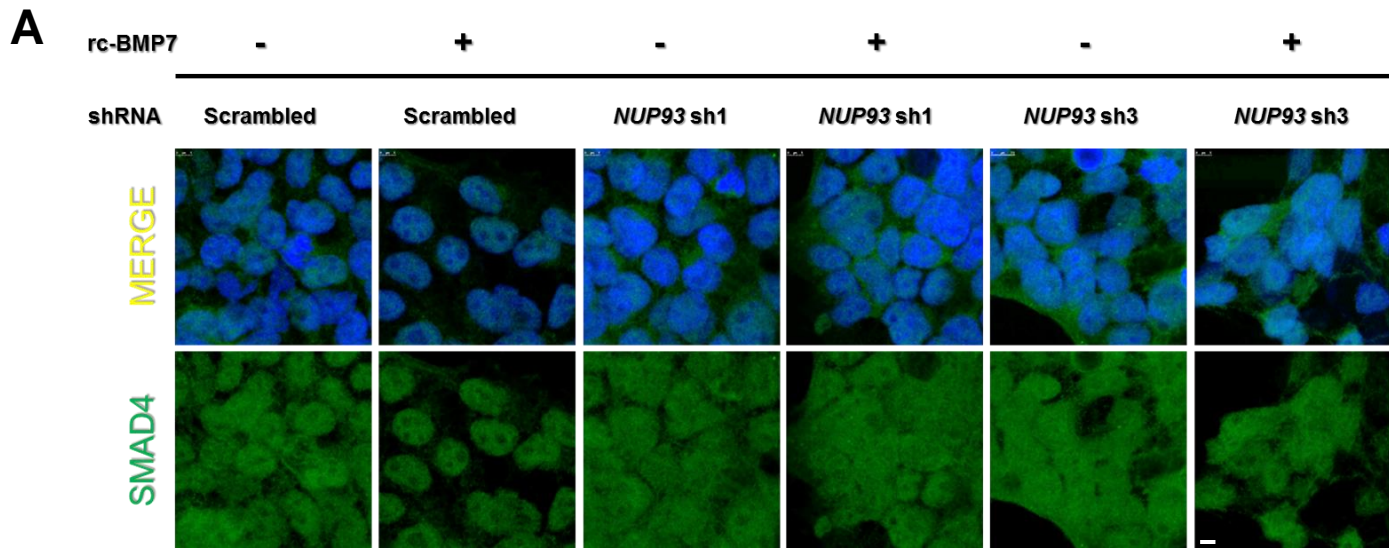
Supplementary Figure 7. NUP93 interacts with NUP205.

GFP tagged NUP205 precipitates Myc tagged NUP93 upon co-overexpression in HEK 293 cells. Mutant clones reflecting alleles of *NUP93* identified in individuals with SRNS do not abrogate the interaction.



Supplementary Figure 8. Myc tagged NUP93 interacts with GFP tagged SMAD4 upon co-expression in HEK293 cells.

Clones reflecting C-terminal mutations identified in individuals with steroid resistant nephrotic syndrome (Lys442Asn_fs*14, Gly591Val, Tyr629Cys) abrogate the interaction.

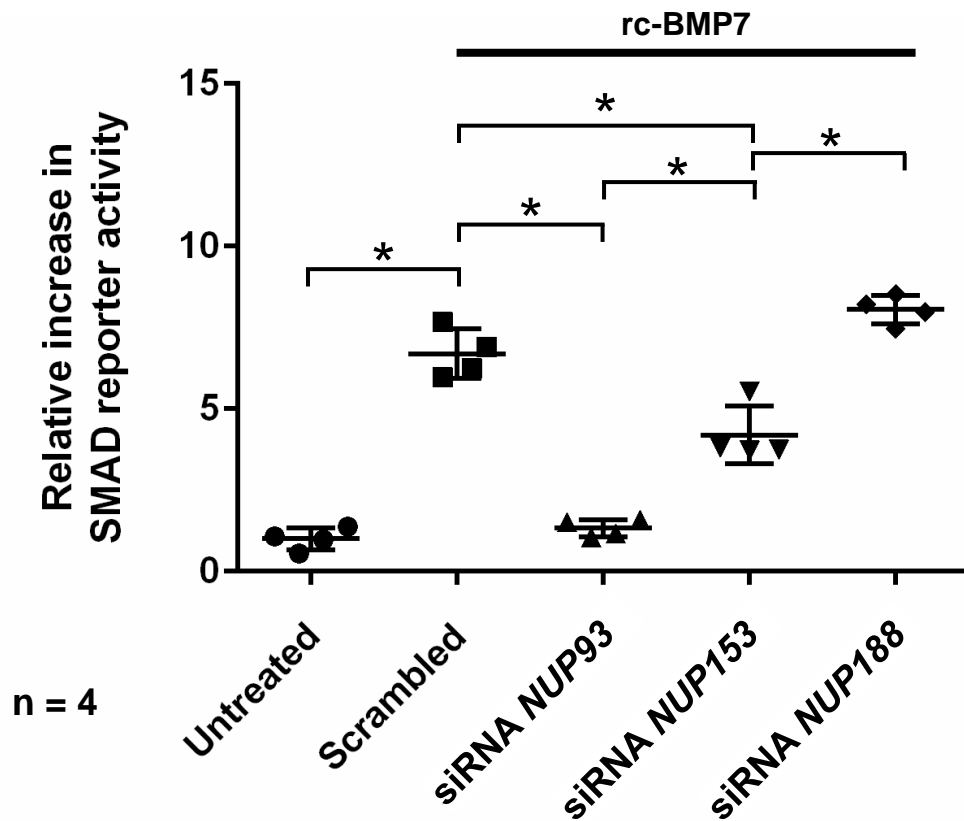


Supplementary Figure 9. Knockdown of *NUP93* interferes with BMP7 induced activation of SMAD signaling.

(A) Upon knockdown of *NUP93* using two different shRNAs in HEK293 cells BMP7 fails to induce efficient translocation of SMAD4 from the cytoplasm to the nucleus compared to negative control (scrambled).

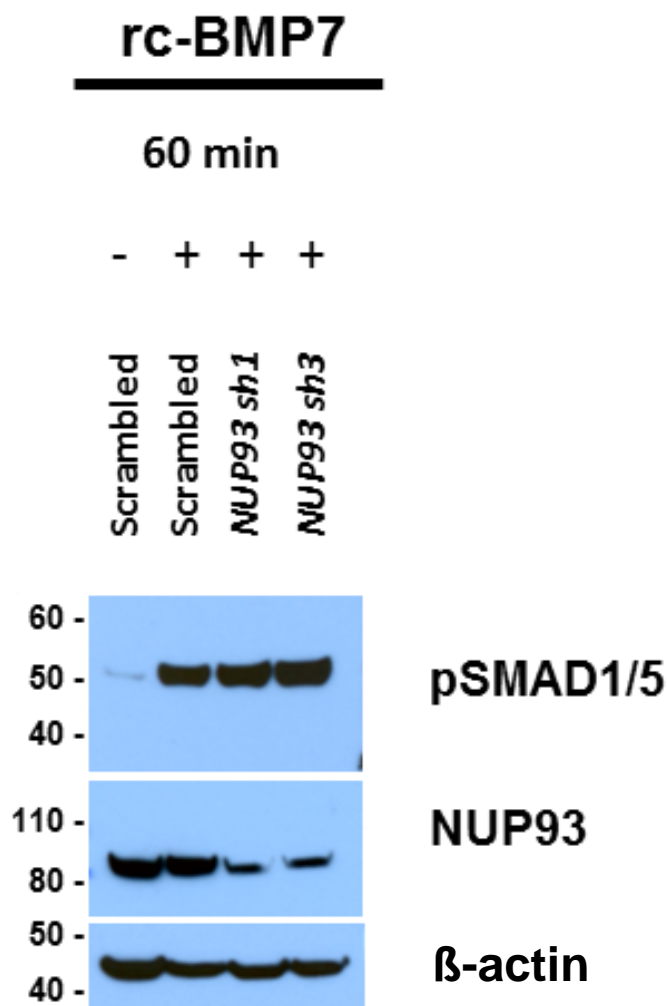
(B) Whereas transfection with wildtype *Nup93* rescues cytoplasmic-to-nuclear translocation of SMAD4 (white arrows), all 5 mutants detected in individuals with SRNS fail to rescue SMAD4 translocation in HEK293 cells.

Scale bars are 5 μ m in **(A)** and 25 μ m in **(B)**.



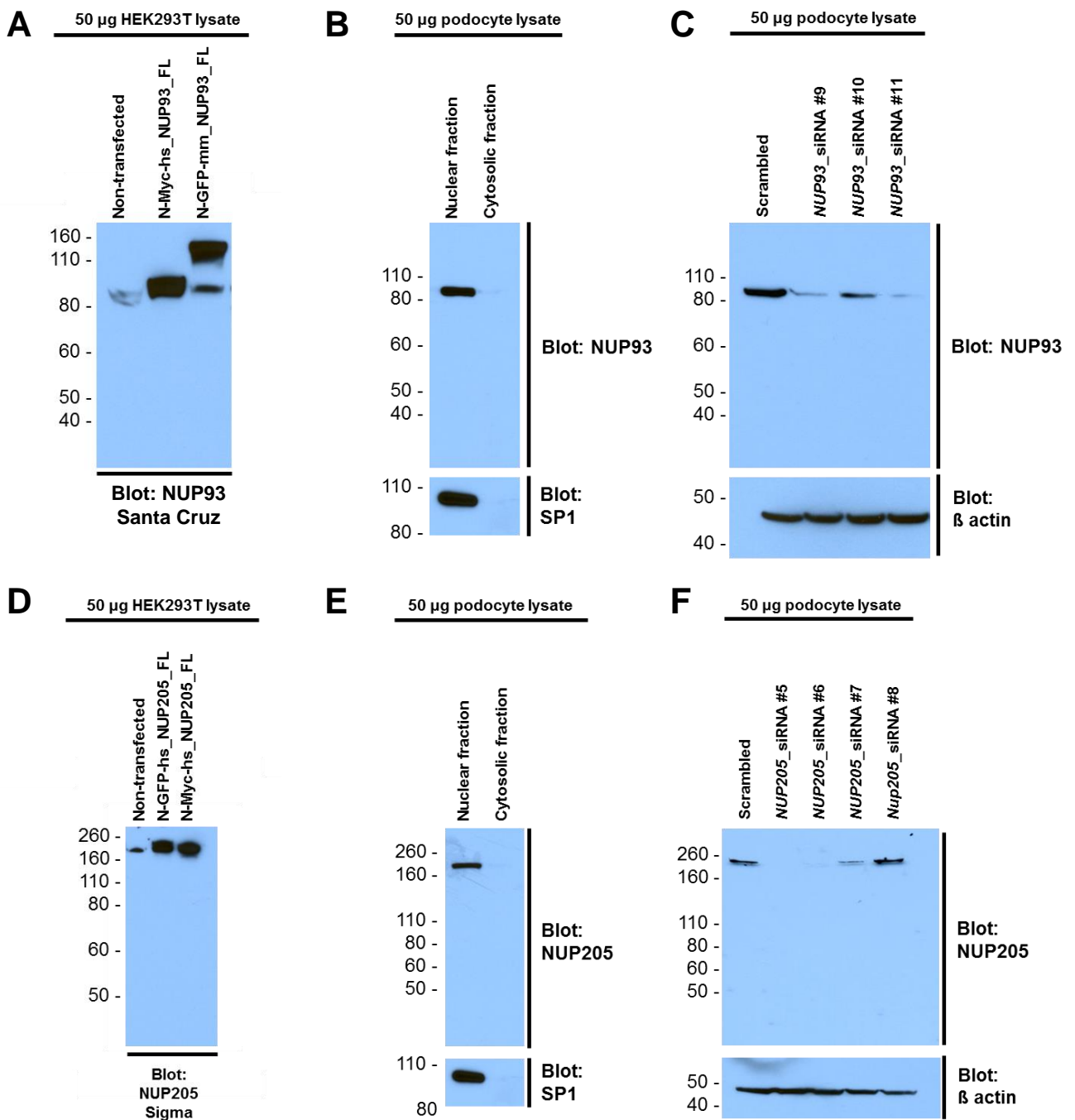
Supplementary Figure 10. Knockdown of *NUP93*, but not *NUP188* decreases SMAD reporter activity upon BMP7 stimulation.

HEK293 cells were transfected with a luciferase reporter constructs under the control of a SMAD responsive promoter allowing to measure SMAD reporter activity in response to BMP7 stimulation (rc-BMP7). Compared to scrambled control siRNA, knockdown of *NUP93* significantly reduces SMAD reporter activity (2nd vs. 3rd lane). Knockdown of *NUP153*, encoding a nuclear basket protein, induces less pronounced, but significant reduction of SMAD reporter activity. Knockdown of *NUP188*, encoding a direct interactor of *NUP93* did not reduce SMAD reporter activity.



Supplementary Figure 11. SMAD1/5 phosphorylation upon BMP7 treatment and *NUP93* knockdown in HEK293 cells.

Treatment of HEK293 cells with recombinant BMP7 induces phosphorylation of SMAD1/5 after 60 minutes (upper panel). Transfection of HEK293 cells with shRNA against human *NUP93* shows efficient knockdown of *NUP93* compared to scrambled control (middle panel). β -actin control (lower panel) confirms equal loading.



Supplementary Figure 12. Characterization of antibodies against NUP93 and NUP205 by immunoblotting.

(A-C) Characterization of the anti NUP93 antibody (mouse, Santa Cruz, sc-374400).

(A) Antibody detects N-terminally Myc tagged full-length human NUP93 (N-Myc-hs_NUP93_FL), as well N-terminally GFP tagged full-length mouse Nup93 (N-GFP-mm_NUP93_FL) upon overexpression in HEK293 cells.

(B) Detection of endogenous NUP93 in the nuclear fraction of human podocytes at the expected relative mobility of 93 kDa.

(C) Knockdown of *NUP93* in human podocytes using 3 different siRNAs demonstrates the specificity of the detected band at ~93 kDa.

(D-F) Characterization of the anti NUP205 antibody (rabbit polyclonal, Sigma, HPA024574).

(D) Antibody detects N-terminally GFP tagged full-length human NUP205 (N-GFP-hs_NUP205_FL), as well N-terminally Myc tagged full-length human NUP205 (N-Myc-hs_NUP205_FL) upon overexpression in HEK293T cells.

(E) Detection of endogenous NUP205 in the nuclear fraction of human podocytes at the expected relative mobility of 205 kDa.

(F) Knockdown of NUP205 in human podocytes using 4 different siRNAs demonstrates the specificity of the detected band at ~205 kDa.

(β -actin and SP1 controls confirm equal loading.)

Supplementary Table 1: RNAi targets and primer sequences

Primer	Target sequence	
Human <i>NUP93</i> , siRNA #9	CGGCAGAUGUCAAGGCGUC	
Human <i>NUP93</i> , siRNA #10	GCUCAAGGAAUAAGCGCAA	
Human <i>NUP93</i> , siRNA #11	AGAGUGAAGUGGGCGGACAA	
Human <i>NUP93</i> , shRNA #1	GCAAGTGAAACAGCGAATTCT	
Human <i>NUP93</i> , shRNA #3	GGACTCCACGTTCTATCTTCT	
Primer	Forward sequence	Reverse sequence
NUP93_ex2	TTGAAACCTGTCTTTCCCTTG	TTCAAGGCAGGAAAGAAGAAAC
NUP93_ex3	TCCAGGTGATGTCTATGGAAAG	TATGCTCTGGGTTCCACCTG
NUP93_ex4	GCTCCAGAATGGAAGAAAC	CCCTCATCTGTATACATCTACATTTTG
NUP93_ex5	CCTGAGGGTCATTGTTCTCTG	CAAATGCGGCATCCTAAAAG
NUP93_ex6	ATCTCATGCCTGCTCTCTTC	TGGCTTAATCCCCCTTAAAATC
NUP93_ex7	CTCCGAGGAAGGAAAGGTTG	ATTTCAACCAAATCGGCAAG
NUP93_ex8	GGTCAGAGTGCCACAAAGAAC	AGCACACCTAGCCTGAGGAC
NUP93_ex9	TGCCCTTCCAAGCTACAGTG	CTGCTCTGGGGGTGTAAGT
NUP93_ex10	GGGGCTTAGCTCGTTTTAG	GAAGGATGCCCTTTGATTC
NUP93_ex11	GGCTTCCCTGCTTTTATGTG	CTATGTGGGCAGGGGAAAC
NUP93_ex12	CCCAGCTCATAACCATAGCC	TGGACAAGAGAAGGGAAAGG
NUP93_ex13	ACCAGTGAGCCCCTTCTTTC	GGGACGTGCTGTGGTTAC
NUP93_ex14	GGTTGTGACCCATTCTGACC	CACTCACACAGCGCAGAAAC
NUP93_ex15	ACCCGGAAGTTTGAGTCCAC	GAAAACCATGGGGAGGAGAG
NUP93_ex16	TTATCCCATTCATCCATTTG	GGGCCATAATTTTCATTCC
NUP93_ex17	TTTGGATCCTAATTGCTTCTCTG	GGGAGGGTGCTACAACAATG
NUP93_ex18	GTTCTCTTTGGTGGGTAGGG	CTTTGAAAGCTGTCTGCTG
NUP93_ex19	AGGCTGGTCACTGACTCCTG	CTGCACTTCAAACACCTTTCC
NUP93_ex20	GAAGCCCTTTGGAGTATGTGAG	CTGAAAGGGAACCACTCTGG
NUP93_ex21	TGTTTCAGTGCCATCAGCTC	ATGTTTCTCGGAATGCTG
NUP93_ex22	ACCCATCAGGGATCTGTCC	CCCATGTGCCTGATGTAAGT

Supplementary Table 1: RNAi targets and primer sequences (continued)

Primer	Forward sequence	Reverse sequence
XPO5_ex2	TTCCTCTCTCTTGGAGATTGC	CTCAGCCCTCGAAAGGAAAC
XPO5_ex3	GAAGTCACGCTTTGCCTAAAC	TTTTGCCATTTCATTGACAG
XPO5_ex4	GAACAGGTTCAATTTGTTCTGTTTG	CCCTGAAGTTTGTCCAAGG
XPO5_ex5	AAGATTAATCAAAAACACTCATATTGG	GCAACAGAAAATAGCCTTTGG
XPO5_ex6	AGGTCATGGCTGCAGTGAG	TTCAAGGGCATTGATTTGTG
XPO5_ex7	CCCAAACCTTTAAATGACTTTCTG	TGTTACCGAGGACTTCATGG
XPO5_ex8	CTTACAGAAGATGTCGGTACTTTG	CAGGAGACGGAGGTTGTGG
XPO5_ex9	CAGGTTTTGCCACCAAATAAG	AAATGGGCTTGAAGCTCTCC
XPO5_ex10	TTCCTCTCCTGCTTTTCTCG	CACTACGGTCATTCCCAAG
XPO5_ex11	CACAGGCTGGTCTCCAATC	TCCAAATCCTTTGACGTTTTC
XPO5_ex12	CAGTGGGTCCACTTTTCATCC	TCTGCAATGGGAAACTAGGG
XPO5_ex13	CTCTCCAGGATGAGCAAAGC	TGATTCCTGTCCTTCCCTTG
XPO5_ex14	TCTGCGATCTTTCAATGCTG	CATTTACAGCTGAGCAACAG
XPO5_ex15	TAAGTGGAGGCGACCATTG	TGGGCAATGTAGCAAGATCC
XPO5_ex17	AGGGCATAACAAGAAACATGG	CTACTTCAGCCAGGGTCCAG
XPO5_ex18	CCTTGAGTAAGCCACCTCTCC	AACCAAAATGGGTGCTTGAG
XPO5_ex19	ACTCCCACGTTTCTACCAG	GCCTGTAACTCCTGTGGAAG
XPO5_ex20	CATTCTCTCTGGCCTCTGTG	AAACAACAGAGAAAAGCCATTATTC
XPO5_ex21	AGGCAGGAAGACTGCTTGAG	CTGCATCAGATGGAAAAGCTC
XPO5_ex22	TCACGTAGCCAATGCTTTG	ATATGGAGAGGCAGCATTGG
XPO5_ex23	CTTCCAGTTCTGCCTCTTCC	AGGGCTGGCAGTAACAGATG
XPO5_ex24	AAGCTCAGAAATGGCCAGAG	CATCTGGCAAATCCTTTAGGG
XPO5_ex25	CATCAGGGATGTGGGATAGG	TTCATCCACCAAGAAGAGTGG
XPO5_ex26	TCAGTGGATCACTGCTGTCC	CCTTCATGGAGTTGGCTGAG
XPO5_ex27	AGACAGGTTGGGATCAGTGG	GTATGATGGAGGCACACAGC
XPO5_ex28	ATGGGCATTATGTGGAGGTG	CCTGGGCAAGGAGTAAAGG
XPO5_ex29	GGCAACAAAACAAACCCATC	TCAGTCTGCATGACCCAAAC
XPO5_ex30	CCCATTCTCAGAGATTGCAC	GGCCCTAAAGCACAGTTGTC
XPO5_ex31	GCCCATACACATGATTTAAGAAGG	CTCAGCCCTCGAAAGGAAAC
XPO5_ex32	TGAGGGCCCAGCATTAAATTCT	GTGGAAAGTGAGGTGGCAGT

Supplementary Table 1: RNAi targets and primer sequences (continued)

Primer	Forward sequence	Reverse sequence
NUP205_ex1	GCAGATTCTGGAGCCTTTTG	GCCCAGAATTAGGGAAAAGC
NUP205_ex2_1	AGATTA AAAAGTAGCTGTGGGTGTAAC	GAAAATTTCTTACCGGATTTTTG
NUP205_ex2_2	GTGGGAAATGCTCTTTGGAG	GCCAGAAGTCCAAGACAAGC
NUP205_ex3	AGGTAACACTTTGGGACCTTG	TTTTGCATTATTTTACCACTGTTTC
NUP205_ex4	CCCCTTAAGCCCTGAGCTAC	TTCAAATTAACCCCTGAAATCC
NUP205_ex5	GCGTTTGCTATACCTATTATTATGAAG	TGTTTCTGCCTCTGAGATTTG
NUP205_ex6_1	TCAGAATTCAGAGGTGACG	TGCATCCAGTGAGCCATTAG
NUP205_ex6_2	GGCTTGCCAGTCACCTTTAG	TGCAAACACAGGAACAGAGC
NUP205_ex7	TGCTCAGATTTTCTGACTTTTGG	TGCTGTTTCTCATAACAAAATTACC
NUP205_ex8	TGACTTTTCTCCATGTA CTGTG	TTTTATTAGTTTTCCAAAACATAAAGCTG
NUP205_ex9	CACTTTAAGACAGTTGCCTGATTTTC	CTGAAATTTTCCAAAGTTAGGG
NUP205_ex10	CCTAACTTTGGAAAATTT CAGGTG	TCATGTTTTCAAGACTCTCTATCACAG
NUP205_ex11	TCTTTATTAGCTAGTCCGTGTTGC	GAACCTAGTTCAAACACCAATGTTTC
NUP205_ex12	TTTTAAATAAAAATTCTGTGCTGTTTTTC	TGTTTGGGGCTCTTAAAATG
NUP205_ex13	TGGAAAGTCTCATTCTTTTTGTG	AAGCCCAACTTTCCACATTG
NUP205_ex14	GGTCCAGTGGGTGAGGTATG	CAACACTGATCAGAAAACCCTTC
NUP205_ex15	TTTTATTACCAAGTTTTCTTTCTTTTTTC	CATGAATTTAGCACCATATACTTTTG
NUP205_ex16	AAGCAAAATGAATTGGGATTTTC	TGACA ACTTGTGTTGAAAGTGACAG
NUP205_ex17	TGCTGTGTCTCTAAATTGAAACTTG	GCTGTTTGCAAGACATGAAGG
NUP205_ex18	AAACTTGT CATTGTCTTGTTTTCC	TTTACTTCATTTCTCTACCTACAAAGG
NUP205_ex19	CACCAAAAATTTTATCACTGTTCC	TTCGTGGGTAGGTTTTACC
NUP205_ex20	CGTAAATACCTAAGCAGGTTTGC	TCTCAATTCCTCTTACCCATCAC
NUP205_ex21	TGTAATTTTGTGTTGTGATTTCTGC	TGACCCATCCATCACATTACC
NUP205_ex22	AATGCAGCAATTCTAAAAGAAAAG	CGGATTTTATCCACAAATGAAAG
NUP205_ex23	TAGGTTGCCAAGGACTGTTTC	TGTTCTTATAAATACGGGAAAATAATG
NUP205_ex24	TTGTTACATGGGAAAATATCTGTTG	AAGCTTCAGATTTGTGCTTGTC
NUP205_ex25	GCACAGGGCTCTTTGATGTAG	TTTCTATACCAGTTCAGAGTTTGGAG
NUP205_ex26	TCAACTGAATATGATGGCTTGC	TCTGAGCCACTTGACACTGC
NUP205_ex27	AATATTTTGGTCTGGAAATTGG	TTTTAGTCTTTTACCAGCAACC
NUP205_ex28	CCTTG TGATTCAATTCCTGTG	CCCAATCGAAAATGGAAAAC
NUP205_ex29_1	CACTCTAATTTGCCCTTGTCC	CCTGTCTTCAAATGAAGTCTAACAG
NUP205_ex29_2	TGTT CACTGACTGCTCACC	CCACCACCTAGGGAGATTAGG
NUP205_ex30	AGTGGGTTTTGCTTCTATTGG	AAGTAACCATCTCCCAATCCAG
NUP205_ex31_1	GTGGGCCTTTGTGTACAAGC	CAAGCATCTCGACAGACCAC
NUP205_ex31_2	AGAAAACCATGTGGGAAAGG	CAAGAAATCCACCCACCTTG
NUP205_ex32	TTGGTAGCATCTACATGTTTTGG	CAGAATGTATGCCACATTAATTTTC
NUP205_ex33	CCCTTG GACATGATTT CAGC	TGACAGGGGCACAGTATGAC
NUP205_ex34	GGAATGTTTTCTCCTTGTGTTGG	CTCTGCCACAACATTAGGAC
NUP205_ex35	TTTCTATTCTCTTCTTTTCAATG	GGCTCTGTTAGCAGTACCAATTTTC
NUP205_ex36	AACAGGTA CTTACAGTCTTTGTAAAATC	TGGGGAGGATGGTATATTTTG
NUP205_ex37	GCCTTAAGGACTGATTCCATTC	TAAAACCTTAGAGAAGTCACATGG
NUP205_ex38	CTTCAAATCTCGATTTTCATGC	AAAAGAAAATACTGCATCTTACTGG
NUP205_ex39	GGAACATTGTTTTATGTCATCACC	CACAGAAGAATCATTCCAATTCC
NUP205_ex40	CATTTATCATGGTGACCTGCTG	TCTCCTTCCACCTGGTTTTG
NUP205_ex41	TTCTTCTCCTCCGAAACTGG	AGCTCTTGATTCACCCAATTC
NUP205_ex43	AGTATTTACATTGAAAGAACCACATTAC	GGAGACAATTCTCCCAATTC